JOURNAL OF VIROLOGY, Dec. 1990, p. 6045–6053
0022-538X/90/126045-09$02.00/0

Vol. 64, No. 12

Analysis of Efficiently Packaged Defective Interfering RNAs of Murine Coronavirus: Localization of a Possible RNA-Packaging Signal

SHINJI MAKINO,[1,2]* KYOKO YOKOMORI,[1] AND MICHAEL M. C. LAI[1]

*Howard Hughes Medical Institute and Department of Microbiology, University of Southern California School of Medicine, Los Angeles, California 90033,[1] and Department of Microbiology, The University of Texas at Austin, Austin, Texas 78712[2]**

Received 18 May 1990/Accepted 14 September 1990

We have previously shown that most of the defective interfering (DI) RNA of mouse hepatitis virus (MHV) are not packaged into virions. We have now identified, after 21 serial undiluted passages of MHV, a small DI RNA, DIssF, which is efficiently packaged into virions. The DIssF RNA replicated at a high efficiency on its transfection into the helper virus-infected cells. The virus released from the transfected cells interfered strongly with mRNA synthesis and growth of helper virus. cDNA cloning and sequence analysis of DIssF RNA revealed that it is 3.6 kb and consists of sequences derived from five discontinuous regions of the genome of the nondefective virus. The first four regions (domains I to IV) from the 5′ end are derived from gene 1, which presumably encodes the RNA polymerase of the nondefective virus. The entire domain I (859 nucleotides) and the first 750 nucleotides of domain II are also present in a previously characterized DI RNA, DIssE, which is not efficiently packaged into virions. Furthermore, the junction between these two domains is identical between the two DI RNAs. The remaining 77 nucleotides at the 3′ end of domain II and all of domains III (655 nucleotides) and IV (770 nucleotides) are not present in DIssE RNA. These four domains are derived from gene 1. In contrast, the 3′-most domain (domain V, 447 nucleotides) is derived from the 3′ end of the genomic RNA and is also present in DIssE. The comparison of primary sequences and packaging properties between DIssE and DIssF RNAs suggested that domains III and IV and part of the 3′ end of domain II contain the packaging signal for MHV RNA. This conclusion was confirmed by inserting these DIssF-unique sequences into a DIssE cDNA construct; the in vitro-transcribed RNA from this hybrid construct was efficiently packaged into virion particles. DIssF RNA also contains an open reading frame, which begins from domain I and ends at the 5′-end 20 bases of domain III. In vitro translation of DIssF RNA and metabolic labeling of the virus-infected cells showed that this open reading frame is indeed translated into a 74-kDa protein. The structures of both DIssE and DIssF RNAs suggest that a protein-encoding capability is a common characteristic of MHV DI RNA.

Mouse hepatitis virus (MHV), a coronavirus, contains a single-stranded, positive-sensed RNA genome of approximately 31 kb (13, 23; H.-J. Lee, C.-K. Shieh, A. E. Gorbalenya, E. V. Koonin, N. La Monica, J. Tuler, A. Bagdzhyadzhyan, and M. M. C. Lai, Virology, in press). The virion is composed of four structural proteins, three of which are integral envelope proteins, including the peplomer-forming S (spike), M (membrane), and HE (hemagglutinin-esterase) proteins. The HE protein of MHV has esterase activity (31) but no hemagglutinin activity (31) and is present only in some, but not all, MHV strains (31). The fourth structural protein, N, is an internal component of the virus. It is a phosphoprotein of 50 kDa (29) and binds to virion RNA (30), forming the helical nucleocapsid of the virion. Each viral protein is synthesized from one of the seven or eight species of virus-specific mRNA, which have a 3′-coterminal, nested-set structure (10, 14) and contain an identical 5′-end leader sequence of 72 to 77 nucleotides (9, 12, 28). The remaining mRNAs presumably encode other virus-specific proteins, which are not detected in the virion. These mRNAs range from 1.8 kb to the genomic size.

When MHV was serially passaged in tissue culture at a high multiplicity of infection, a variety of defective interfering (DI) RNAs of different sizes was detected (15, 19). Different DI RNAs can be grouped into two types, which are produced at different passage levels (15). One is DI RNA of nearly genomic size, which is efficiently packaged into virus particles. This type of DI RNA (termed DIssA) contains multiple small deletions in almost every viral gene except the 5′-most gene (gene 1), which encodes the putative RNA polymerase, and the 3′-most 1.7 kb, which encodes N protein (15). This type of DI RNA apparently encodes all of the proteins essential for its own RNA replication and can replicate itself even in the absence of a helper virus (17). This DI RNA has a weak, homologous interference activity (17). The second type of DI RNA is detectable in DI particle-infected cells in large quantity, but only a trace amount of it is packaged into virions (17). The packaged DI RNA, though present in only a small amount, serves as the template for its own replication, which occurs at a very fast rate (17). One of this type of DI RNA, DIssE, which is the smallest DI RNA detected so far, consists of three noncontiguous genomic regions, representing the first 0.86 kb from the 5′ end, an internal 0.75 kb of gene 1, and 0.6 kb from the 3′ end of the parental MHV genome (18). This sequence contains a large open reading frame (ORF), from which two proteins were translated (18); however, the function of these proteins is not known.

It has not been clear why the small DI RNAs are not packaged efficiently into MHV virions. The failure of these DI RNAs to be packaged is reminiscent of the properties of

* Corresponding author.

MHV subgenomic mRNAs. One explanation is that both DI and subgenomic mRNAs are too small to be packaged. Alternatively, they may lack a specific RNA-packaging signal. Curiously, both the 5'- and 3'-end sequences of the DI RNA and subgenomic mRNAs are identical to those of the genomic RNA, which is efficiently packaged. Thus, the possible RNA-packaging signal may be localized somewhere within the 5'-most gene (gene 1) but not in the leader sequence, since the latter is present in all of the MHV mRNAs.

In this paper, we report the detection and characterization of a small DI RNA species of 3.6 kb, which is efficiently packaged into MHV virions. By comparing this RNA with DIssE RNA, which is not packaged efficiently, we have localized the packaging signal of MHV RNA to be within the internal 1.5-kb regions of gene 1.

MATERIALS AND METHODS

Viruses and cells. The JHM strain of MHV (MHV-JHM) was originally obtained from the Microbiological Associates, Bethesda, Md. It was plaque cloned three times in DBT cells (19) before being used as virus stocks. The virus stock used in this study had been passaged 21 times undiluted in DBT cells, as previously described (15, 19). This virus stock was further passaged nine times in DBT cells for a total of 30 passages. The plaque-cloned A59 strain of MHV (MHV-A59) was used as a helper virus. Mouse L2 cells (10) were used for RNA transfection. Propagation of viruses was done in DBT cells.

Purification of viruses. Viruses were labeled with $^{32}P_i$ and harvested at 14 h postinfection, according to the published procedures (17). After clarification by low-speed centrifugation, the supernatants were then placed on discontinuous sucrose gradients consisting of 10 and 50% (wt/wt) sucrose in NTE buffer (0.1 M NaCl, 0.01 M Tris hydrochloride [pH 7.2], and 0.001 M EDTA). After centrifugation at 26,000 rpm for 3 h at 4°C in a Beckman SW 28.1 rotor, the virus band at the interphase between 10 and 50% sucrose was collected, diluted with NTE buffer, and centrifuged in a 10 to 60% continuous sucrose gradient at 26,000 rpm for 19 h at 4°C. After centrifugation, fractions were collected from the bottom of the centrifuge tubes and examined for radioactivity. Each fraction was then diluted with NTE buffer and pelleted by centrifugation at 40,000 rpm for 1 h at 4°C in a Beckman SW41 rotor.

Preparation of virion RNA and intracellular RNA. Virion RNA was extracted from the purified viruses by the published procedure (19). For extraction of the intracellular virus-specific RNA, a monolayer culture of infected DBT cells was labeled with $^{32}P_i$ from 6 to 9 h postinfection in the presence of 2.5 μg of dactinomycin per ml. Cytoplasmic extracts were prepared by lysing the cells in NTE buffer containing 0.5% Nonidet P-40. After removal of the nuclei by centrifugation at 15,000 rpm for 20 s, the cytoplasmic extract was incubated with 100 μg of proteinase K per ml in the presence of 1% sodium dodecyl sulfate (SDS) for 30 min at 37°C. RNA was then extracted with phenol-chloroform and precipitated with ethanol. For cDNA cloning of DIssF RNA, poly(A)-containing RNA was collected by oligo(dT)-cellulose column chromatography prior to electrophoresis (20).

Agarose gel electrophoresis. RNA was separated by electrophoresis on 1% agarose gels after denaturation with 1 M glyoxal (22). For preparative gel electrophoresis, RNA was separated on 1% low-melting-point agarose gels without prior treatment with glyoxal (16). The RNA was extracted from the gel slice according to published procedures (16).

cDNA cloning of DIssF RNA. cDNA cloning followed the previously described procedure with slight modifications (4, 18). First-strand cDNA synthesis was performed by using oligo$(dT)_{12-18}$ as a primer and gel-purified DIssF RNA as a template. The second-strand DNA was synthesized by procedures described previously (4, 18). After completion of second-strand cDNA synthesis, the double-stranded DNAs were ligated to *Bam*HI linkers and inserted into *Bam*HI site of plasmid pTZ18U (United States Biochemical Corp.). The recombinant DNAs were transformed into *Escherichia coli* DH5α competent cells (Stratagene) and screened by colony hybridization (26) using a complete cDNA clone of DIssE as a probe (16). Colonies yielding a strong signal were further analyzed by Southern hybridization (21).

PCR. To obtain cDNA clones corresponding to the 5' region of DIssF, polymerase chain reaction (PCR) was utilized. The gel-purified DIssF RNA was mixed with oligonucleotide 101 (5'-CGCTCTTAACTAGTTTGTCC-3'), which is complementary to the sequence of the DIssF RNA at approximately 1.5 kb from the 5' end. After reverse transcription (18), one-fifth of the total reaction mixture was mixed with oligonucleotide 52 (5'-AAGCTTAATACGACT CACTATAGTATAAGAGTGATTGGCGTCCGTAC-3') (16), which contains the T7 promoter sequence followed by the 5' end sequence of MHV genomic RNA, and incubated at 93°C for 60 s, 37°C for 40 s, and 72°C for 100 s in PCR buffer (0.05 M KCl, 0.01 M Tris hydrochloride [pH 8.3], 0.0025 M $MgCl_2$, 0.01% gelatin, 0.17 mM (each) dNTPs, and 5 U of *Taq* polymerase [Perkin Elmer-Cetus]). After 20 cycles of reaction, the PCR product of 1.5 kb was purified from the agarose gel and used for cloning.

DNA and RNA sequencing. DNA sequencing was carried out by the dideoxyribonucleotide chain termination method, as described previously (25). The dideoxyribonucleotide chain termination method, after adaptation for RNA sequencing (32), was used for RNA sequencing.

Plasmid construction. The procedures for the construction of the DIssE-DIssF hybrid plasmids are diagrammed in Fig. 1. The 1.9-kb *Ppu*MI-*Spe*I fragment of clone BA 114, representing the 3' portion of DIssF RNA, was inserted into the *Ppu*MI-*Spe*I site of the complete DIssE cDNA clone of DE5-w4 (16). This construct was designated DF1-2. The DF1-2 DNA was digested with *Pvu*I, treated with T4 DNA polymerase, and then digested with *Sph*I. The 2.0-kb *Pvu*I-*Sph*I cDNA fragment was ligated with the *Sph*I-*Sca*I fragment (4.0 kb) of DE5-w4, yielding plasmid MP44, which contains a 1.6-kb internal fragment of DIssF.

RNA transcription and transfection. Plasmid DNAs were linearized by *Xba*I digestion and transcribed with T7 RNA polymerase as previously described (16). RNA transfection was performed by the DEAE-dextran method (16, 17).

In vitro translation. An mRNA-dependent rabbit reticulocyte lysate (Promega) was used as previously described (27).

Labeling of intracellular proteins, imunoprecipitation, and SDS-PAGE. Labeling of intracellular proteins, immunoprecipitation, and SDS-polyacrylamide gel electrophoresis (PAGE) were performed as previously described (18).

RESULTS

Efficient packaging of DIssF RNA into MHV virion. We have previously studied various intracellular DI RNA species detected during the first 20 passages of MHV-JHM (15, 19). Among these DI RNAs, only the largest one, DIssA,

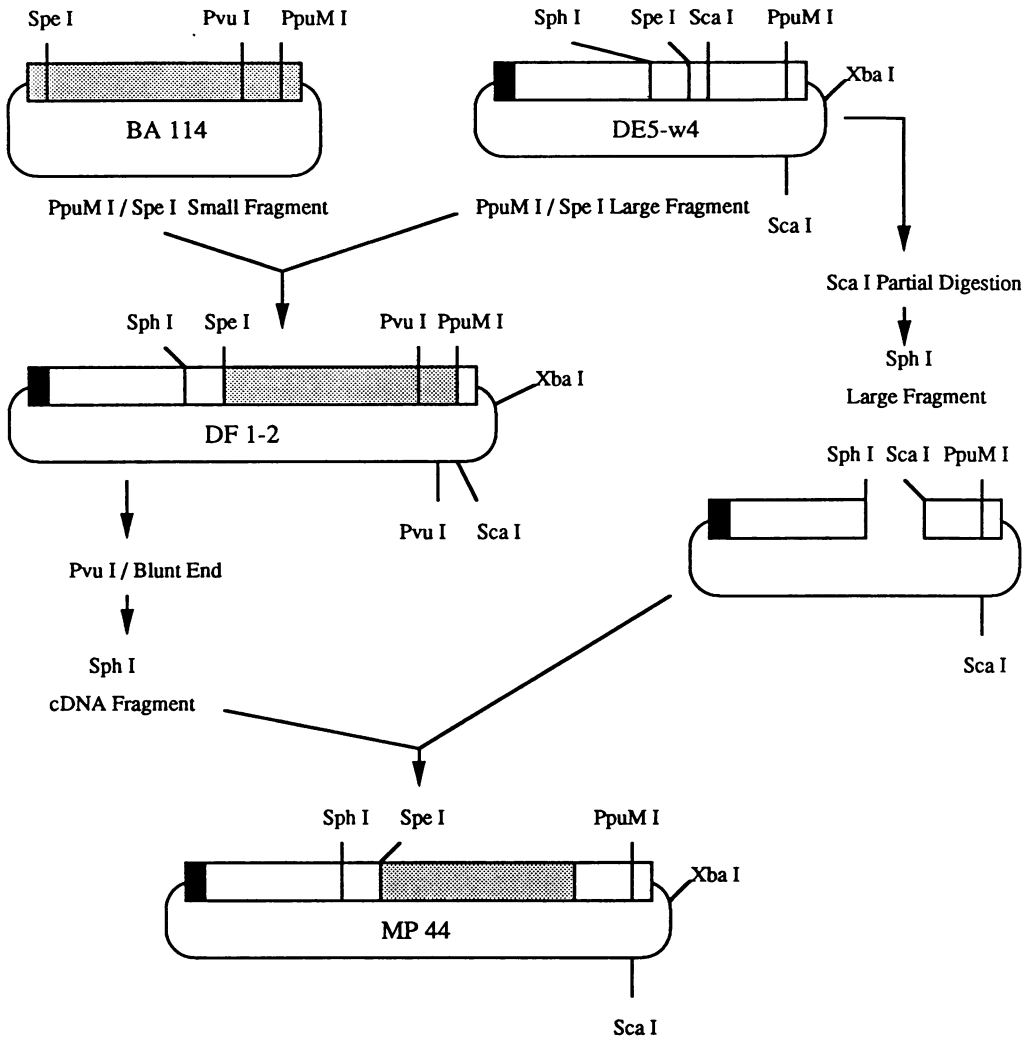

FIG. 1. Construction of the clones DF1-2 and MP44 of MHV DI cDNAs. The details of each step are described in Materials and Methods. The open boxes and shaded boxes represent sequences derived from DIssE and DIssF, respectively. The black boxes indicate T7 promoter.

was efficiently packaged into MHV virions, while other DI RNA species, e.g., DIssB1, DIssB2, DIssC, DIssD, and DIssE, were not packaged efficiently (15, 19). At passage level 21, a new DI RNA species, DIssF, became the predominant DI RNA (15). To examine whether this DI RNA was packaged into MHV virions, ^{32}P-labeled MHV-JHM at passage level 30 was purified. Care was taken to ensure that virus particles of lower density, which may contain DI RNA, were included. A single peak of radioactivity was detected, which had the same buoyant density as the nondefective virus (Fig. 2A). Viral RNA was extracted from each fraction of the sucrose gradient and analyzed by agarose gel electrophoresis. In the peak fractions containing virions, both the virion genomic RNA and DIssF RNA were present (Fig. 2B). The distribution of DIssF RNA was identical to that of the genomic RNA. Furthermore, the DIssF RNA from the purified virions comigrated with the DIssF RNA from infected cells (Fig. 2C). The amount of DIssF RNA in virions was much higher than that of the corresponding DIssE RNA in virions found in previous studies (compare Fig. 2B, lane 9, of this study with Fig. 1, lane C, of reference 17). Densitometry analysis of various RNA species in the virion demonstrated that the molar ratio between DIssF RNA and the genomic-sized RNA in the virion was approximately 1. Thus, we conclude that DIssF RNA was as efficiently packaged as the genomic RNA into MHV virions.

Homologous interference by DIssF RNA. We have previously demonstrated that the smallest MHV DI RNA, DIssE, did not appreciably inhibit mRNA synthesis or virus production of helper virus (16, 17). This low level of interference activity is probably due to the poor packaging efficiency of DIssE RNA; thus, only a small proportion of cells was infected with DIssE-containing DI particles. Since DIssF RNA was efficiently packaged into MHV virion, we predicted that DIssF-containing DI particles would have greater homologous interference activity toward helper virus. To test this prediction, 0.5 μg of the gel-purified, nondenatured DIssF RNA was transfected into monolayers of mouse L2 cells which had been infected with MHV-A59 1 h prior to transfection (17). The virus harvested from the transfected L2 cells was then passaged on DBT cells. The infectious virus titer at each passage level was assayed. It was found that at the third passage, the virus infectivity decreased drastically (Fig. 3A). Subsequently, the virus titer fluctuated with each additional virus passage. Such a fluctuation of infectious virus titer was consistently observed in three

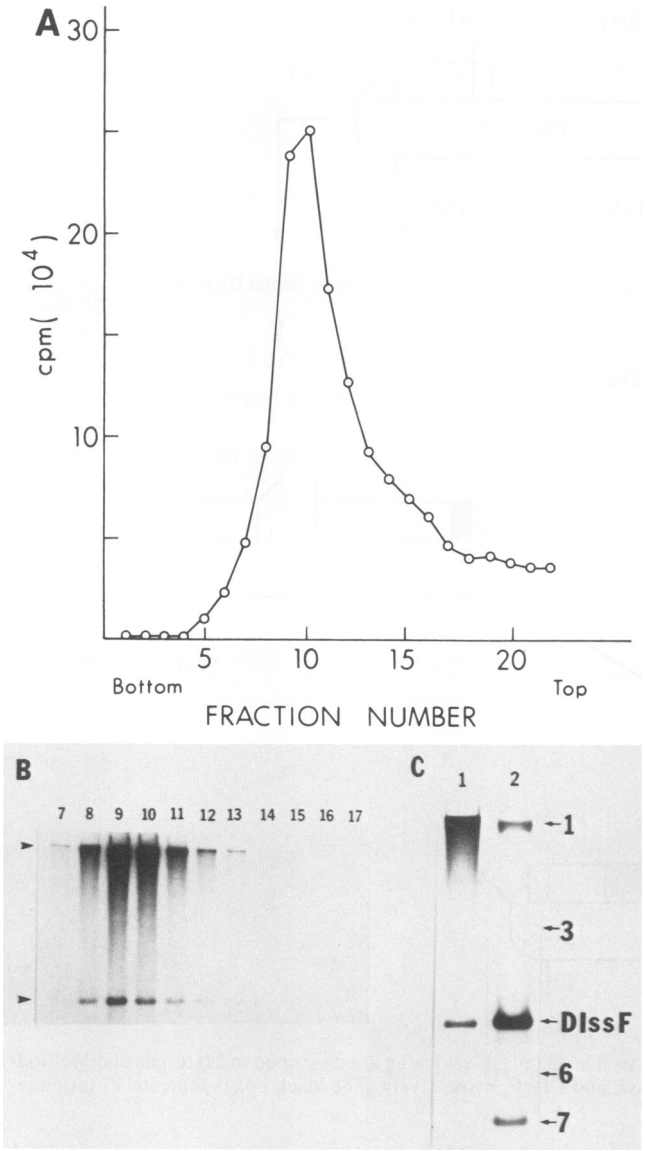

FIG. 2. Sucrose gradient sedimentation of DIssF RNA-containing MHV-JHM. (A) ^{32}P-labeled virus released from DBT cells infected with MHV-JHM (passage level 30) was purified by 10 to 60% sucrose gradient sedimentation at 26,000 rpm for 19 h in a Beckman SW 28.1 rotor. Fractions (600 μl) were collected. Portions of each fraction were analyzed for radioactivity. (B) Agarose gel electrophoresis of glyoxal-denatured virion RNAs extracted from each fraction shown in panel A. Numbers at the top of each lane represent fraction numbers. The genomic RNA and DIssF RNA are indicated by arrowheads. (C) Agarose gel electrophoresis of glyoxal-denatured ^{32}P-labeled virion RNA (lane 1) and intracellular RNAs (lane 2) from DBT cells infected with MHV-JHM (passage level 30). The positions of virus-specific mRNA species (1, 3, 6, and 7) and DIssF RNA are indicated.

independent experiments. This pattern of virus fluctuation is consistent with the classical DI virus interference pattern (24). The virus samples obtained from mock- or DIssE-transfected cells were also passaged in parallel. In both cases, there was no significant decrease of virus infectivity during the first three passages, even though DIssE RNA replicated to a high level at each passage (data not shown). Beginning at the fourth passage, however, the virus titers of both mock- and DIssE-transfected cells decreased, corresponding to the appearance of a new DI RNA species which comigrated with the DIssA RNA species (data not shown). This phenomenon was consistently observed in three independent experiments. The nature of this new DI RNA was not further studied. To confirm that DIssF RNA has a high level of homologous interference activity, DBT cells were coinfected with MHV-A59 and the DIssF-containing DI particles which had undergone two passages following RNA transfection; the growth of MHV-A59 in coinfected cells was then compared with that from cells infected only with MHV-A59. The growth of MHV-A59 was strongly (99.6%) inhibited by DIssF-containing DI particles. By contrast, DIssE-containing DI particles did not interfere with the multiplication of MHV-A59 (data not shown). These results demonstrated that DIssF RNA has a high level of homologous interference activity.

The interference activity of DIssF RNA was also examined at the level of intracellular mRNA synthesis (Fig. 3B). At passage 3, DIssF RNA was the only RNA detected in the cells coinfected with DIssF-containing virus and MHV-A59; the synthesis of mRNAs of helper virus was almost completely inhibited. No other DI RNA species was generated, even after additional DIssF passages (data not shown). This result suggests that DIssF RNA is a highly interfering DI RNA. In contrast, DIssE RNA did not inhibit the synthesis of helper virus mRNAs, probably because it was poorly packaged into virions (17, 18).

The primary structure of DIssF RNA. We next studied the primary structure of DIssF RNA. Sequence analysis was performed with DIssF cDNA clones and PCR products. The 5′-most end of DIssF was also examined by direct RNA sequencing by using a specific primer (5′-CGCCGAATGGA CACGTC-3′) complementary to nucleotides 172 to 188 from the 5′ end of the genome of MHV-JHM (27). Sequence analysis revealed that DIssF RNA consists of five noncontiguous regions (Fig. 4). The first four regions (domains I through IV) are derived from MHV gene 1. The first domain represents 859 nucleotides from the 5′ end of the genomic RNA. The second domain, 827 nucleotides, corresponds to the region at 3.1 to 3.9 kb from the 5′ end of the genomic RNA. Domain I and most of the domain II of DIssF are also present in DIssE, and the junction between these two domains is identical to that of DIssE (18); however, DIssF contains 77 more nucleotides than DIssE at the 3′ region of domain II. Domains III (655 nucleotides) and IV (770 nucleotides) correspond to the regions at 7.0 to 7.7 kb and 19.7 to 20.5 kb from the 5′ end of the genomic RNA, respectively (23; H.-J. Lee et al., in press). These two domains are not present in the DIssE RNA. The 3′-most domain (domain V) represents 447 nucleotides from the 3′ end of the MHV-JHM genome. Domain V of DIssF is shorter by 155 nucleotides at the 5′ end than the corresponding region of DIssE (18).

The entire sequence of DIssF is almost identical to that of the corresponding regions of MHV genomic RNA, with some exceptions. There are five nucleotide substitutions in domain II and six substitutions within the leader region (Fig. 5) (1). Three of the six nucleotide substitutions (nucleotides 12, 31, and 32) in the leader sequence were also detected in the DIssE RNA (18). In addition, nine nucleotides (UUUAU AAAC) were deleted in DIssF at the junction between the leader RNA and the remaining genomic sequences.

Identification of the packaging signal. Sequence comparison between DIssE and DIssF RNAs showed that DIssF contained sequences in domains III and IV and part of the 3′ end of domain II that are not present in DIssE. These

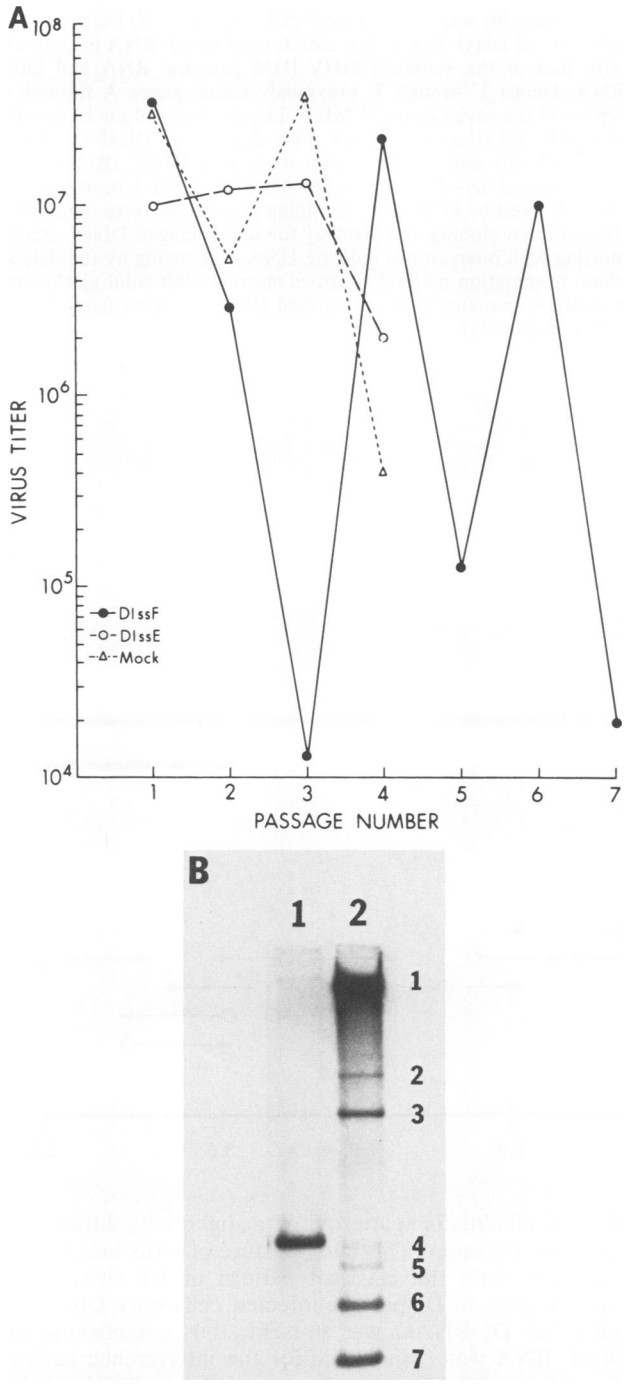

FIG. 3. Virus production and mRNA synthesis of DIssF-containing MHV-A59. (A) Infectious virus titers (PFU/0.2 ml). L2 cells were infected with MHV-A59 (at a multiplicity of infection of 5) and then mock transfected, transfected with 0.5 μg of purified DIssF RNA, or transfected with 0.5 μg of purified DIssE RNA in the presence of DEAE-dextran (18). The culture fluid of infected cells was harvested at 14.5 h postinfection and then passaged without dilution on DBT cells. The virus titer at passage 1 represents the infectivity of virus which was grown once in DBT cells. (B) Agarose gel electrophoresis of intracellular RNA. ^{32}P-labeled virus-specific RNA from DBT cells infected with MHV-A59 (passage 2) obtained from DIssF-transfected cells (lane 1) or mock-transfected cells (lane 2) was denatured with glyoxal and electrophoresed on a 1% agarose gel.

sequences could contain RNA-packaging signals. To examine this possibility, two cDNA clones, MP44 and DF1-2, which contain most of the DIssF-unique sequences and DIssE RNA sequences, were constructed (Fig. 1). The possible packaging of these DI RNAs was then examined.

The MP44 clone was derived from a DIssE-specific DE5-w4 clone but contains the DIssF sequence from nucleotide 1489 to 3089, which includes all of domain III, a portion from the 3′ end of domain II, and almost all of domain IV (except its 3′-most 20 nucleotides). It has deleted the 5′-most 12 nucleotides of the third domain of DIssE (Fig. 4). The other clone, DF1-2, was derived by inserting the DIssF sequence from nucleotide 1489 to 3437 into DIssE cDNA clone DE5-w4. DF1-2 is very similar to DIssF, except for several nucleotide changes in the leader sequence and domain II, since domains I and II of DIssF are closely related to those of DIssE. The plasmids were linearized by *Xba*I and transcribed by T7 RNA polymerase in the presence of a cap analog [m^{7}G(5′)ppp(5′)G]. The RNA was transfected into monolayers of mouse L2 cells which had been infected with MHV-A59 1 h prior to transfection. The virus was harvested from the transfected L2 cells 14 h postinfection and passaged one time on DBT cells. The virus released from this DBT cell culture was then used to infect fresh DBT cells and was labeled with $^{32}P_i$. ^{32}P-labeled RNA was extracted from purified virus particles and analyzed by agarose gel electrophoresis. The DI RNAs derived from both DF1-2 and MP44 constructs were efficiently packaged into MHV virions (Fig. 6). These data clearly demonstrated that these three DIssF-unique domains contain the packaging signal.

Translation of DIssF RNA in vitro and in vivo. Sequence analysis of DIssF RNA reveals the presence of a single, large ORF. This ORF consists of domains I and II and the 5′ portion of domain III. The first 215 amino acids correspond to the N terminus of the MHV gene 1 product, part of which was cleaved to become a p28 protein (1, 3, 27). The ensuing 276 amino acids were derived from the region at 3.1 to 3.9 kb from the 5′ end of the genome. Since domain II of DIssF has 77 nucleotides more than the corresponding region of DIssE, the DIssF RNA encodes an extra 25 amino acids in domain II. There were five nucleotide substitutions in this domain; as a result, two amino acids were converted from Arg to Lys at position 248 and from Val to Ala at position 273 (Fig. 5). However, the sequence substitutions at nucleotides 1193 and 1194 did not alter the amino acids encoded. The last six amino acids at the C terminus of this ORF are encoded from domain III and utilize a reading frame which is different from that utilized by the MHV genomic RNA. As a result, the ORF in DIssF is terminated 21 nucleotides downstream from the junction site between domains II and III. The predicted molecular weight of this ORF product is 54,670.

To examine whether the ORF of DIssF RNA was functional, the synthesis of DIssF-specific protein in DI particle-infected cells was examined. DBT cells were mock infected (Fig. 7A, lane 1), infected with MHV-A59 (Fig. 7A, lane 2), or infected with DIssF-containing MHV-A59 (passage 2) (Fig. 7A, lane 3). A specific, 74-kDa protein was detected in the DI particle-infected cells. Since this protein was larger than the predicted protein, the DIssF-specific nature of this protein was further confirmed by in vitro translation. The DIssF RNA was purified from DI particle-infected cells and then translated in rabbit reticulocyte lysates. A 74-kDa protein was obtained which was identical in size to the protein found in the infected cells (Fig. 7A, lane 4). This protein was immunoprecipitated with anti-p28 antibody (1) (Fig. 7B). Four minor protein species were also immunopre-

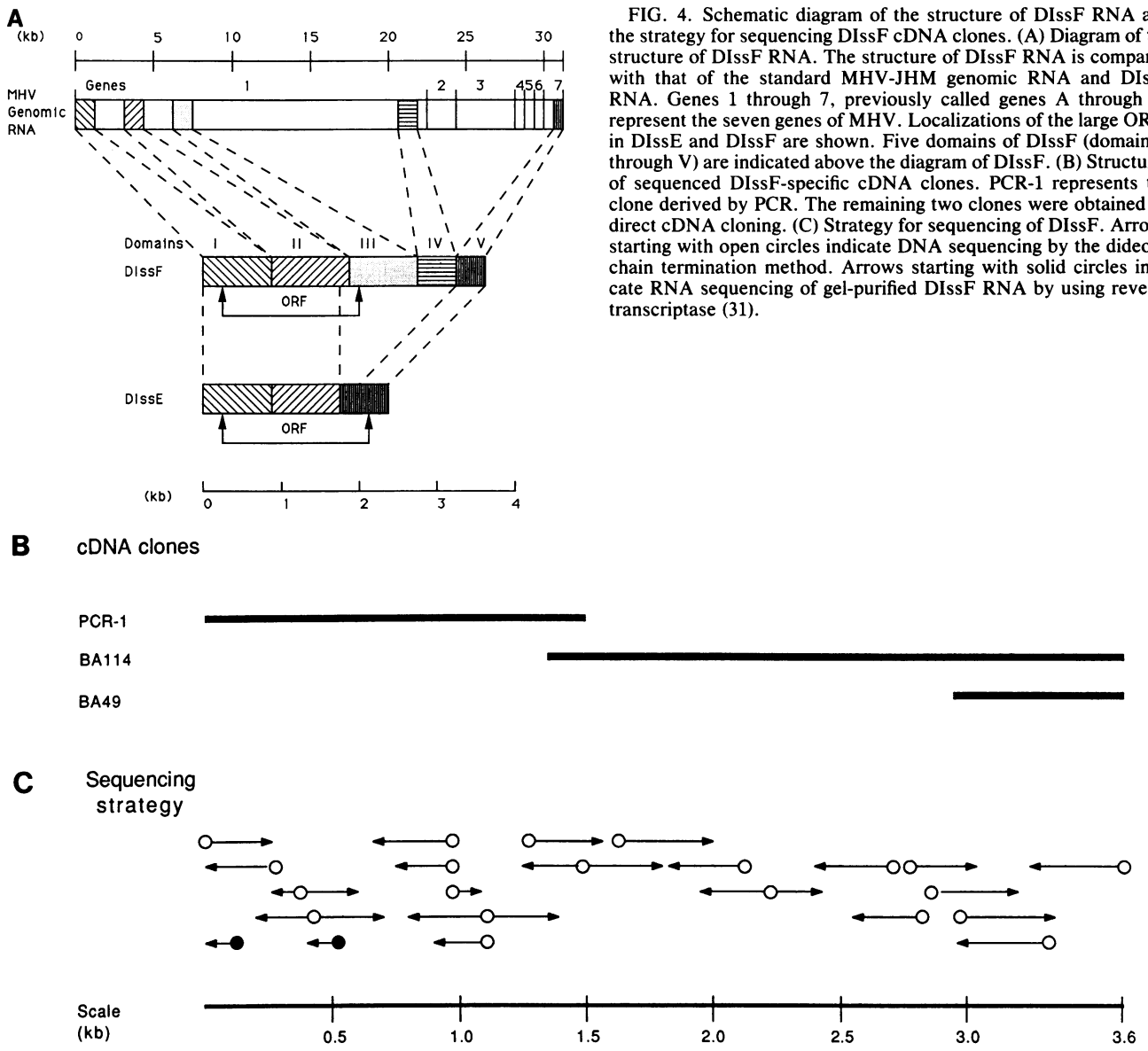

FIG. 4. Schematic diagram of the structure of DIssF RNA and the strategy for sequencing DIssF cDNA clones. (A) Diagram of the structure of DIssF RNA. The structure of DIssF RNA is compared with that of the standard MHV-JHM genomic RNA and DIssE RNA. Genes 1 through 7, previously called genes A through G, represent the seven genes of MHV. Localizations of the large ORFs in DIssE and DIssF are shown. Five domains of DIssF (domains I through V) are indicated above the diagram of DIssF. (B) Structures of sequenced DIssF-specific cDNA clones. PCR-1 represents the clone derived by PCR. The remaining two clones were obtained by direct cDNA cloning. (C) Strategy for sequencing of DIssF. Arrows starting with open circles indicate DNA sequencing by the dideoxy chain termination method. Arrows starting with solid circles indicate RNA sequencing of gel-purified DIssF RNA by using reverse transcriptase (31).

cipitated by the anti-p28 antibody; the origin of these proteins is not known. From these data, we conclude that DIssF is a functional mRNA and translates a 74-kDa protein. The size deviation of the DI-specific proteins from their predicted molecular masses could not be explained at this time and has also been observed with DIssE-specific protein (18).

DISCUSSION

The present study identified a new class of MHV DI RNA which is subgenomic and yet packaged efficiently into virions. Efficient packaging of DIssF RNA was unambiguously demonstrated by several lines of evidence. First, a large amount of DIssF RNA was present in the purified MHV virion. Second, DI particles containing DIssF RNA showed a strong interference activity with the replication and mRNA synthesis of helper viruses. This strong interference activity can be explained if the majority of the virus-infected cells were also infected with the DIssF-containing DI particles. Third, virus samples from the DIssF-transfected cells showed a fluctuating pattern of virus infectivity during serial undiluted passages. This cyclic nature of virus infectivity is consistent with the classical pattern of DI viruses (24). Furthermore, in DI particle-infected cells only DIssF, but not other DI RNAs, was present, thus establishing that DIssF RNA was responsible for the interference activity. Since the molar ratio of the genomic RNA to DIssF RNA in the virions was approximately 1, the packaging efficiency of DIssF RNA should be almost the same as that of the genomic RNA.

It is interesting that the DIssF RNA-containing virus particles had the same buoyant density as the infectious virus, despite the fact that DIssF RNA is 3.6 kb whereas the MHV genomic RNA is 31 kb. This large difference in RNA size could have altered the buoyant density of the virus particles, as demonstrated for the DI particles of vesicular stomatitis virus (7). One possible explanation is that the DIssF RNA was copackaged with MHV genomic RNA into the same virus particle, whereas another possibility is that

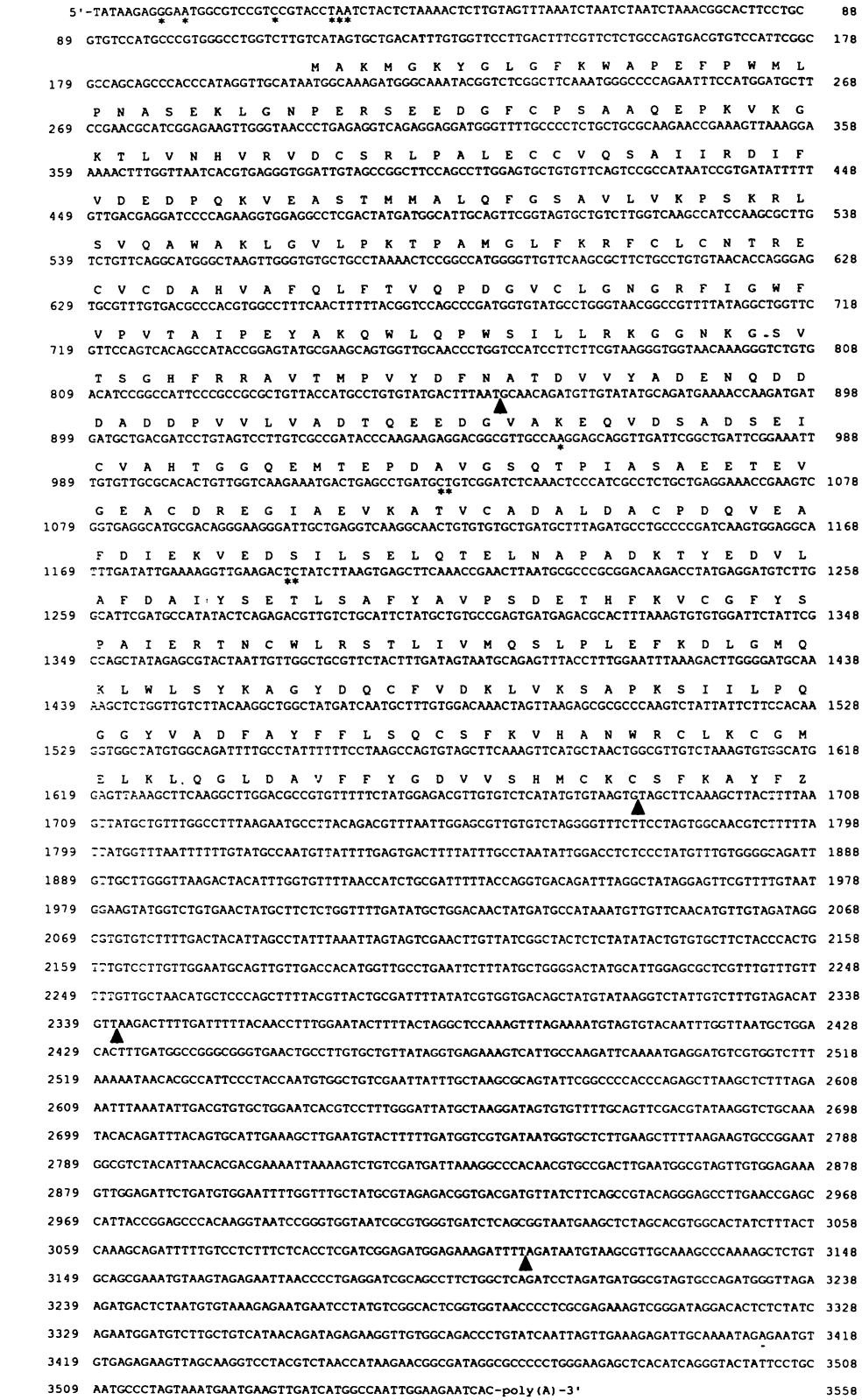

FIG. 5. DNA sequence and deduced amino acid sequence of the DIssF cDNA clones. A translation of the main ORF is shown as single-letter amino acids. Solid triangles indicate the sites where fusion of discontiguous sequences occurred. The base substitutions in DIssF compared with the parental MHV-JHM RNA are indicated by asterisks.

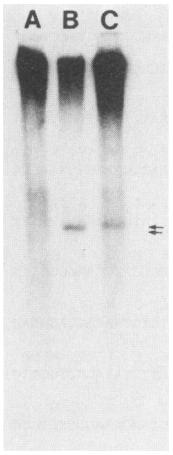

FIG. 6. Agarose gel electrophoresis of glyoxal-denatured ^{32}P-labeled virion RNA from DI particle-infected cells. Viruses at passage level 1 from mock-transfected (A), DF1-2 DI RNA-transfected (B), and MP44 DI RNA-transfected (C) cells were used for infection. DI RNAs are indicated by arrows.

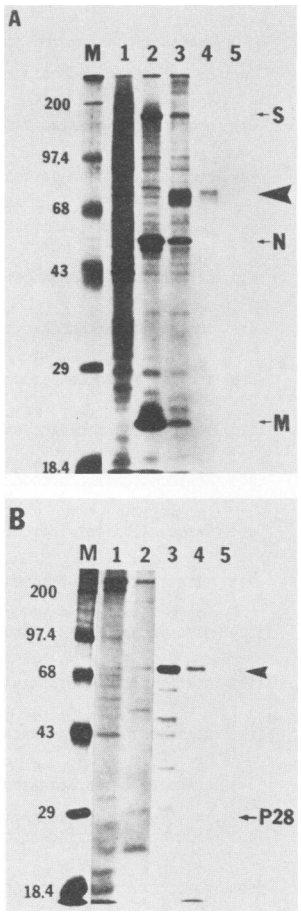

FIG. 7. Translation of the DIssF-specific protein. (A) Polyacrylamide gel electrophoresis of proteins from DI particle-infected cells (lanes 1 to 3) and in vitro translation products of gel-purified DIssF RNA in a rabbit reticulocyte lysate (lanes 4 and 5). DBT cells were mock infected (lane 1) or infected with MHV-A59 (lane 2) or with MHV-A59 (passage 2) obtained from DIssF-transfected cells (lane 3). At 8 h postinfection, cultures were labeled with [^{35}S]methionine for 20 min, and the cytoplasmic lysates were prepared and analyzed by SDS-PAGE. Lanes 4 and 5 are ^{35}S-labeled in vitro translation products of the gel-purified DIssF and no RNA, respectively. MHV-A59-specific structural proteins are indicated as S, N, and M. The DIssF-specific protein is indicated by an arrowhead. Lane M, ^{14}C-labeled marker proteins. (B) Immunoprecipitation of the proteins by anti-p28 serum. ^{35}S-labeled samples shown in panel A were immunoprecipitated with anti-p28 serum and analyzed by SDS-PAGE. The order of samples is the same as that in panel A. Lanes 1 and 2 were exposed much longer than other lanes in order to detect p28.

several molecules of DIssF RNA were packaged together into a virion. Our preliminary study examining the effects of serial virus dilution on the synthesis of DIssF RNA in the DI particle-infected cells has ruled out the first possibility (unpublished observation).

Of the two naturally occurring subgenomic DI RNA species characterized so far, DIssF is efficiently packaged whereas DIssE is not. Thus, the extra sequence present in DIssF RNA may contain the packaging signal for MHV RNA. The existence of such a packaging signal was suggested from the finding that other DI RNAs or mRNAs of various sizes, which are either larger or smaller than or are equivalent to DIssF RNA, were not packaged. From the common structure of these DI RNAs and mRNAs, it can be deduced that the RNA-packaging signal must be present within gene 1, which encompasses 22 kb (23; H.-J. Lee et al., in press), but is outside the leader sequence. It is evident that the nucleotide substitutions in domain II of DIssF were not responsible for the high level of packaging efficiency of DIssF RNA, because DF1-2 DI RNA, in which the substituted nucleotides were converted to sequences similar to those of DIssE RNA, was efficiently packaged (Fig. 6). In addition, the nine-nucleotide deletion (UUUAUAAAC) at the junction between the leader and the remaining DI sequence in DIssF RNA (11, 18, 26) was also not likely to be responsible for the high level of packaging efficiency of DIssF RNA, since DIssE has this deletion but is not packaged, whereas the nondefective genomic RNA does not have the deletion and yet is packaged. Rather, the extra sequence present in DIssF, which includes the 3′-end 77 nucleotides of domain II and domains III and IV, is most likely responsible for the specific RNA packaging. Analysis of the MP44 DI RNA, which contains most of these regions, conclusively demonstrated that the packaging signal resides within these three separate regions in gene 1 of no more than 1,480 nucleotides in total. This is the first identification of the packaging signal in coronavirus RNA. This packaging signal may interact with the N protein during the first step of viral morphogenesis. Experiments using deletion mutants of DIssF RNA are needed to further define this signal.

Both DIssE and DIssF RNAs contain an ORF, which can be translated into proteins in vitro and in vivo. Puzzlingly, both of these proteins had lower electrophoretic mobilities than expected from the predicted protein sizes. Whether this anomaly of electrophoretic mobility was due to posttranslational modifications or unusual amino acid compositions of the DI-specific proteins is not clear. The function of these proteins is currently unknown. It is interesting to note that poliovirus DI RNAs also contain functional ORFs (2, 5, 8). It is possible that protein synthesis is necessary for the initiation of DI RNA replication or for interaction with other host-derived or helper virus-derived proteins. Alternatively, these proteins may interact with DI RNA itself in *cis* to regulate DI RNA replication. Analyses of additional DI

RNAs will likely shed further light on the functional significance of DI-specific proteins.

ACKNOWLEDGMENTS

We thank Chien-Kou Shieh for performing some of the preliminary work and for valuable suggestions during the course of this study. We also thank Susan Baker and Jennifer Fosmire for helpful comments on the manuscript.

M.M.C.L. is an investigator at the Howard Hughes Medical Institute. This work was supported in part by Public Health Service grants AI 19244, AI 29984, and NS 18146 from the National Institutes of Health.

LITERATURE CITED

1. **Baker, S. C., C.-K. Shieh, L. H. Soe, M.-F. Chang, D. M. Vannier, and M. M. C. Lai.** 1989. Identification of a domain required for autoproteolytic cleavage of murine coronavirus gene A polyprotein. J. Virol. **63**:3693–3699.
2. **Cole, C. N., and D. Baltimore.** 1973. Defective interfering particles of poliovirus. II. Nature of the defect. J. Mol. Biol. **76**:325–343.
3. **Denison, M. R., and S. Perlman.** 1986. Translation and processing of mouse hepatitis virus virion RNA in a cell-free system. J. Virol. **60**:12–18.
4. **Gubler, U., and B. J. Hoffman.** 1983. A simple and very efficient method for generating cDNA libraries. Gene **25**:263–269.
5. **Hagino-Yamagishi, K., and A. Nomoto.** 1989. In vitro construction of poliovirus defective interfering particle. J. Virol. **63**: 5386–5392.
6. **Hirano, N., K. Fujiwara, S. Hino, and M. Matsumoto.** 1974. Replication and plaque formation of mouse hepatitis virus (MHV-2) in mouse cell line DBT culture. Arch. Gesamte Virusforch. **44**:298–302.
7. **Holland, J. J., S. I. T. Kennedy, B. L. Semler, C. L. Jones, L. Roux, and F. A. Grabau.** 1980. Defective interfering RNA viruses and the host-cell response, p. 137–192. *In* H. Frankel-Conrat and R. R. Wagner (ed.), Comprehensive virology, vol. 16.
8. **Kaplan, C. T., and V. R. Racaniello.** 1988. Construction and characterization of poliovirus subgenomic replicons. J. Virol. **62**:1687–1696.
9. **Lai, M. M. C., R. S. Baric, P. R. Brayton, and S. A. Stohlman.** 1984. Characterization of leader RNA sequences on the virion and mRNAs of mouse hepatitis virus, a cytoplasmic RNA virus. Proc. Natl. Acad. Sci. USA **81**:3626–3630.
10. **Lai, M. M. C., P. R. Brayton, R. C. Armen, C. D. Patton, C. Pugh, and S. A. Stohlman.** 1981. Mouse hepatitis virus A59: mRNA structure and genetic localization of the sequence divergence from hepatotropic strain MHV-3. J. Virol. **39**:823–834.
11. **Lai, M. M. C., S. Makino, L. H. Soe, C.-K. Shieh, J. G. Keck, and J. O. Fleming.** 1987. Coronavirus: a jumping RNA transcription. Cold Spring Harbor Symp. Quant. Biol. **52**:359–365.
12. **Lai, M. M. C., C. D. Patton, R. S. Baric, and S. A. Stohlman.** 1983. Presence of leader sequences in the mRNA of mouse hepatitis virus. J. Virol. **46**:1027–1033.
13. **Lai, M. M. C., and S. A. Stohlman.** 1978. RNA of mouse hepatitis virus. J. Virol. **26**:236–242.
14. **Leibowitz, J. L., K. C. Wilhelmsen, and C. W. Bond.** 1981. The virus-specific intracellular RNA species of two murine coronaviruses: MHV-A59 and MHV-JHM. Virology **114**:39–51.
15. **Makino, S., N. Fujioka, and K. Fujiwara.** 1985. Structure of the intracellular defective viral RNAs of defective interfering particles of mouse hepatitis virus. J. Virol. **54**:329–336.
16. **Makino, S., and M. M. C. Lai.** 1989. High-frequency leader sequence switching during coronavirus defective interfering RNA replication. J. Virol. **63**:5285–5292.
17. **Makino, S., C.-K. Shieh, J. G. Keck, and M. M. C. Lai.** 1988. Defective-interfering particles of murine coronaviruses: mechanism of synthesis of defective viral RNAs. Virology **163**:104–111.
18. **Makino, S., C.-K. Shieh, L. H. Soe, S. C. Baker, and M. M. C. Lai.** 1988. Primary structure and translation of a defective interfering RNA of murine coronavirus. Virology **166**:550–560.
19. **Makino, S., F. Taguchi, and K. Fujiwara.** 1984. Defective interfering particles of mouse hepatitis virus. Virology **133**:9–17.
20. **Makino, S., F. Taguchi, N. Hirano, and K. Fujiwara.** 1984. Analysis of genomic and intracellular viral RNAs of small plaque mutants of mouse hepatitis virus, JHM strain. Virology **139**:138–151.
21. **Maniatis, T., E. F. Fritsch, and J. Sambrook.** 1982. Molecular cloning: a laboratory manual. Cold Spring Harbor Laboratory, Cold Spring Harbor, N.Y.
22. **McMaster, G. K., and G. G. Carmichael.** 1977. Analysis of single- and double-stranded nucleic acids on polyacrylamide and agarose gels by using glyoxal and acridine orange. Proc. Natl. Acad. Sci. USA **74**:4835–4838.
23. **Pachuk, C. J., P. J. Bredenbeek, P. W. Zoltick, W. J. M. Spaan, and S. R. Weiss.** 1989. Molecular cloning of the gene encoding the putative polymerse of mouse hepatitis virus, strain A59. Virology **171**:141–148.
24. **Palma, E. L., and A. S. Huang.** 1974. Cyclic production of vesicular stomatitis virus caused by defective interfering particle. J. Infect. Dis. **129**:402–410.
25. **Sanger, F., S. Nicklen, and A. R. Coulson.** 1977. DNA sequencing with chain-terminating inhibitors. Proc. Natl. Acad. Sci. USA **74**:5463–5467.
26. **Shieh, C.-K., L. H. Soe, S. Makino, M.-F. Chang, S. A. Stohlman, and M. M. C. Lai.** 1987. The 5'-end sequence of the murine coronavirus genome: implications for multiple fusion sites in leader-primed transcription. Virology **156**:321–330.
27. **Soe, L. H., C.-K. Shieh, S. C. Baker, M.-F. Chang, and M. M. C. Lai.** 1987. Sequence and translation of the murine coronavirus 5'-end genomic RNA reveals the N-terminal structure of the putative RNA polymerase. J. Virol. **61**:3968–3976.
28. **Spaan, W., H. Delius, M. Skinner, J. Armstrong, P. Rottier, S. Smeekens, B. A. M. van der Zeijst, and S. G. Siddell.** 1983. Coronavirus mRNA synthesis involves fusion of non-contiguous sequences. EMBO J. **2**:1939–1944.
29. **Stohlman, S. A., and M. M. C. Lai.** 1979. Phosphoproteins of murine hepatitis virus. J. Virol. **32**:672–675.
30. **Sturman, L. S., K. V. Holmes, and J. Behnke.** 1980. Isolation of coronavirus envelope glycoproteins and interaction with the viral nucleocapsid. J. Virol. **33**:449–462.
31. **Yokomori, K., N. La Monica, S. Makino, C.-K. Shieh, and M. M. C. Lai.** 1989. Biosynthesis, structure, and biological activities of envelope protein gp65 of murine coronavirus. Virology **173**:683–691.
32. **Zimmern, D., and P. Kaesburg.** 1978. 3'-Terminal nucleotide sequence of encephalomyocarditis virus RNA determined by reverse transcriptase and chain terminating inhibitors. Proc. Natl. Acad. Sci. USA **75**:4257–4261.